Am J Physiol Heart Circ Physiol
282: H110–H121, 2002.

Effects of CPAP therapy on cardiovascular variability in obstructive sleep apnea: a closed-loop analysis

VASILY BELOZEROFF, RICHARD B. BERRY,
CATHERINE S. H. SASSOON, AND MICHAEL C. K. KHOO
Biomedical Engineering Department, University of Southern California, Los Angeles, California 90089; Department of Medicine, University of Florida, Gainesville, Florida 32610; and Department Of Medicine, University of California-Irvine/Veterans Affairs Medical Center, Long Beach, California 90822

Received 26 April 2001; accepted in final form 11 September 2001

Belozeroff, Vasily, Richard B. Berry, Catherine S. H. Sassoon, and Michael C. K. Khoo. Effects of CPAP therapy on cardiovascular variability in obstructive sleep apnea: a closed-loop analysis. *Am J Physiol Heart Circ Physiol* 282: H110–H121.—To determine the long-term effects of continuous positive airway pressure (CPAP) therapy on cardiovascular variability, we measured R-R interval (RR), systolic blood pressure (SBP) and respiration (ΔV) in 13 awake, supine patients with moderate-to-severe obstructive sleep apnea (OSA), before and after ~6 mo of treatment. Using these data, we estimated the dynamics of the following components of a closed-loop circulatory control model: *1*) the baroreflex component, *2*) the neural coupling of ΔV to RR or respiratory sinus arrhythmia (RSA), *3*) the mechanical effects of respiration (MER) on SBP, and *4*) the circulatory dynamics (CID) component, which is responsible for the feed-forward effect of RR fluctuations on SBP. Baroreflex and RSA gains increased whereas MER and CID gains decreased in compliant subjects whose average CPAP use was >3 h/night. In contrast, baroreflex, RSA, and MER gains remained unchanged and CID gain increased in noncompliant subjects. Other summary measures were unchanged in both groups, except for mean RR, which increased in compliant patients. Closed-loop analysis provides a simple but sensitive means for quantitatively assessing cardiovascular control in OSA by using data collected from a single, nonintrusive test procedure.

heart rate variability; blood pressure regulation; sleep-disordered breathing; baroreflex sensitivity; respiratory sinus arrhythmia; mathematical model; autonomic function

THERE IS A GROWING BODY of evidence (35, 44) that suggests a causal link between obstructive sleep apnea (OSA) and cardiovascular disease. Although the exact mechanisms that underlie this relationship remain unresolved, the acute cardiovascular effects of repetitive upper airway obstruction in sleep are well established. The alternating cycles of OSA and subsequent arousals with accompanying hyperpnea produce large fluctuations in intrathoracic pressure and recurring episodes of hypoxia and hypercapnia. These periodic events lead to dramatic alterations in hemodynamics and elevations in catecholamine level and sympathetic neural activity (43, 44). The neural and humoral consequences of nocturnal apnea carry over into wakefulness in the daytime (7, 12). Increased sympathetic drive is believed to be responsible for the elevated heart rate, decreased heart rate variability (HRV) and increased blood pressure variability observed in alert patients with moderate-to-severe OSA (26, 36). The nocturnal application of continuous positive airway pressure (CPAP) over several months has been found to reduce muscle sympathetic nerve activity and plasma catecholamine levels (14, 27, 42) and to increase heart rate variability (34). Consistent with these changes, autonomic stress tests also demonstrate improvements in cardiovascular function (41). Furthermore, daytime blood pressure is lowered significantly in hypertensive OSA patients after long-term CPAP therapy (22).

Although the monitoring of autonomic function provides an objective and noninvasive means of quantifying the effectiveness of long-term CPAP therapy in patients with OSA, there are practical disadvantages associated with existing measures. For instance, measurements of muscle sympathetic nerve activity require considerable technical expertise and are highly susceptible to artifactual noise introduced by limb movement. Moreover, microneurography gives only a regionally confined assessment of sympathetic tone, which can be quantitatively different in the heart and various parts of the vasculature (20). The mean ± SD values of heart rate and blood pressure are summary statistical measures, conveying information that reflects only the net effect of all the factors that contribute to cardiovascular control, thus providing little insight into the underlying physiological mechanisms. Power spectral analysis of HRV and blood pressure variability offers a promising avenue for investigating the dynamics of cardiovascular autonomic function (19). However, this type of analysis is carried out in the

Address for reprint requests and other correspondence: M. C. K. Khoo, Biomedical Engineering Dept., Univ. of Southern California, OHE-500, University Park, CA 90089-1451 (E-mail: khoo@bmsrs.usc.edu).

The costs of publication of this article were defrayed in part by the payment of page charges. The article must therefore be hereby marked "*advertisement*" in accordance with 18 U.S.C. Section 1734 solely to indicate this fact.

frequency domain and provides little information about the temporal relationships that link dynamic changes in blood pressure to changes in heart rate. Also, they do not directly take into account the powerful influence of changes in respiration.

In this study, we propose an alternative method for quantifying the effects of long-term CPAP therapy on cardiovascular variability in OSA. Our approach takes the form of a closed-loop model of cardiovascular control, with respiration as an external input. Such a model enables the characterization of the dynamic interrelationships between various pairings of the three measured variables: respiration, heart rate, and arterial blood pressure. Furthermore, the causal structure of the model allows us to computationally "open the loop" of the closed-loop system, thereby separating the feedforward from the feedback components. Spectral analysis does not permit this kind of temporal delineation. Finally, closed-loop analysis provides a means for obtaining a comprehensive assessment of the functional mechanisms that contribute toward HRV and blood pressure variability, using data measured from a single test procedure.

METHODS

Subjects. Thirteen male patients with moderate-to-severe OSA were studied before (preCPAP) and after (postCPAP) CPAP therapy. The overall duration of CPAP therapy was 184 ± 15 (SE) days. In each subject, diagnosis of OSA was confirmed in a prior sleep study (9) using standard polysomnographic instrumentation. Criteria for admission to the study included an apnea-hypopnea index (AHI) >20/h and the selection of CPAP as the prescribed therapy. Exclusion criteria included diabetes, significant cardiac arrhythmia, congestive heart failure, and lung disease. The apnea-hypopnea index during CPAP application was found to be 3.5 ± 0.8/h in this group of patients. Five subjects were hypertensive. For safety, these subjects continued antihypertensive medication between initial and followup studies. Three patients were on felodopine whereas the other two used diltiazem. Informed consent was obtained from all subjects. The study was approved by the Long Beach Veterans Affairs Medical Center Research Committee.

In each of the subjects, the CPAP device (model Aria LX; Respironics; Pittsburgh, PA) employed contained a memory chip for storing the duration and pressure level at which the unit was in use. After the repeat study, compliance information was obtained by downloading the time at prescribed pressure from the memory chip with the use of vendor-supplied software (Encore Data Management; Respironics). Compliance with the prescribed therapy was assessed by evaluation of the average nightly CPAP use in each subject. Because compliance varied widely across individuals, we divided the subjects into two groups: the six compliant subjects (*group C*) who used CPAP for an average of >3 h per night, and the seven noncompliant subjects (*group N*), whose average nightly CPAP use was <3 h. A previous study (13) has shown that use of CPAP therapy for an average of 3.4 h per night over a duration of 4 wk leads to improved daytime cognitive performance. Hers et al. (15) found that application of CPAP in the first 4 h of sleep resulted in a significant reduction of the severity of OSA over the remainder of the night, during which treatment was not applied. A recent study (23) of CPAP compliance in 1,155 OSA patients reported that subjects who used CPAP <2 h per night in the first 3 mo were unlikely to continue with treatment for >1 year. For these reasons, we felt that the cutoff value of 3 h per night constituted a reasonable dividing line between the compliant and noncompliant groups.

Table 1 shows the characteristics of these two groups of subjects. The differences in age, body mass index, AHI, and prescribed CPAP levels between the two groups were not statistically significant. Furthermore, there were no significant changes in body mass index before and after CPAP therapy in both groups. Application of Fisher's exact test showed that the ratio of subjects in each group who were hypertensive was not different between groups. However, although *group N* used CPAP less, the total duration of CPAP therapy in these subjects was significantly longer ($P < 0.05$). The variability in times between studies was due primarily to patient accessibility: for example, *subject C5* had to be restudied after only 3 mo due to impending relocation to another city, whereas *subject N4* was studied after ~9 mo because he was temporarily lost to followup.

Table 1. *Patient characteristics*

Group	Subject No.	Age, yr	Hypertensive?	BMI, kg/m²		AHI, h	Prescribed CPAP, cmH_2O	Duration of Therapy, days	Average Nightly CPAP Usage, h
				PreCPAP	PostCPAP				
Compliant subjects: avg. nightly CPAP use >3 h	*C1*	38	N	37.3	36.5	67.6	10	133	8.27
	C2	54	Y	41.4	44.8	153.5	14	154	7.65
	C3	48	N	39.3	40.7	75	12	217	7.41
	C4	63	N	37.3	35.9	42.2	8	133	6.55
	C5	36	N	32.9	33.4	105.7	10	91	3.60
	C6	52	Y	32.1	30.7	83	10	189	3.43
	Means ± SE	48.5 ± 4.2		36.7 ± 1.5	37.0 ± 2.1	87.8 ± 15.6	10.7 ± 0.8	153 ± 18	6.15 ± 0.86
Noncompliant subjects: avg. nightly CPAP use <3 h	*N1*	39	Y	38.0	36.7	113.8	14	237	1.55
	N2	55	N	25.8	26.5	43.4	10	202	1.27
	N3	47	Y	33.3	33.3	69.1	7	233	1.22
	N4	50	N	29.1	29.4	45.5	8	279	0.83
	N5	34	N	28.5	28.1	25	10	132	0.24
	N6	54	Y	28.1	27.4	26	9	174	0.01
	N7	30	N	38.7	40.3	53.5	10	222	0.00
	Means ± SE	44.1 ± 3.7		31.6 ± 1.9	31.7 ± 2.0	53.8 ± 11.6	9.7 ± 0.8	211 ± 18	0.73 ± 0.24

Values are means ± SE. BMI, body mass index; CPAP, continuous positive airway pressure; *C*, compliant; *N*, noncompliant.

Experimental procedures and data preprocessing. Breathing was monitored using calibrated respiratory inductive plethysmography (Respitrace, Ambulatory Monitoring; Ardsley, NY). Calibration of the respiratory inductive plethysmograph was performed against a spirometer with the subject breathing spontaneously in the supine position. Arterial blood pressure was monitored continuously using finger arterial plethysmography (Finapres model 2350, Ohmeda; Boulder, CO). The electrocardiogram (ECG) was measured using a single bipolar lead and amplified using a bioamplifier (model BMA-831, CWE; Ardmore, PA).

At the start of each study, the subject lay supine while his ECG, blood pressure, and spontaneous respiration were monitored for ~5 min. He was then asked to control his breathing pattern so that it tracked the respiratory waveform measured in the previous 5 min. Both target and tracking waveforms were displayed on a computer monitor. This procedure allowed the subject to become familiarized with the task of tracking the displayed breathing pattern. Finally, the subject was asked to control his breathing pattern so that it tracked a waveform with respiratory durations that varied randomly from breath to breath. The sequence of randomized breath durations employed in our protocol was generated from an algorithm that assumed a stationary Poisson noise process. However, the tidal volumes of the target breath pattern were selected so that the average minute ventilation could be maintained at an approximately constant level equal to that deduced from the subject's previously monitored spontaneous breathing pattern. This ensured that chemical drive would remain relatively unchanged over the course of the procedure. The purpose of employing a randomized breathing pattern was to improve the accuracy with which the model parameters could be estimated, because such a pattern effectively broadens the bandwidth of the "input" (i.e., respiration) (17). The entire randomized breathing protocol was designed to last 5 min. Selection of the 5-min test duration was based partly on preliminary experiments, which showed that tracking performance generally deteriorated when longer random breath sequences were employed. Furthermore, it was important for subsequent analysis to ensure that stationarity in the heart rate and blood pressure measurements were preserved (39). During each procedure, the respiratory signal was digitized at 10 Hz while ECG and blood pressure were sampled at 200 Hz; all signals were recorded and stored in an IBM-compatible computer using custom-designed software based on the Matlab programming environment (Mathworks; Natick, MA).

To extract an R-R interval (RR) time series from each dataset, the time locations of the QRS complexes in the ECG tracing were first detected using a computer algorithm. The results of this procedure were then reviewed manually and edited when necessary to ensure that no detection errors were made. Subsequently, the intervals between successive QRS complexes were computed. Because these spikes occur at irregular intervals, each sequence of RR was converted into an equivalent uniformly spaced time-series (sampling rate: 2 Hz) using a resampling algorithm closely similar to that of Berger et al. (5). Systolic (SBP) and diastolic (DBP) values were also extracted on a beat-by-beat basis via computer algorithm from the continuous blood pressure waveform. The breathing waveform was resampled at 2 Hz so that each respiratory value would be synchronized with the corresponding resampled RR, SBP, and DBP values. Each resampled sequence contained 600 data points (5 min). Before further analyses were performed, very-low-frequency trends were removed from each dataset by fitting and subtracting polynomial functions of up to the fifth order.

Modeling and parameter estimation. A schematic block diagram of the model employed in our analysis is displayed in Fig. 1. Fluctuations in RR [$\Delta RR(t)$] are assumed to be produced by two physiological mechanisms. The first is the baroreflex through which fluctuations in SBP [$\Delta SBP(t)$] lead to changes in heart rate. The second mechanism is the direct coupling between respiration [$\Delta V(t)$] and $\Delta RR(t)$, which accounts largely for what is generally referred to as respiratory sinus arrhythmia (RSA). It should be noted that fluctuations in heart rate that occur around the breathing frequency can also be baroreflex mediated as a result of respiratory-induced changes in arterial blood pressure. The preceding assumptions are represented mathematically by the following equation

$$\Delta RR(t) = \sum_{i=0}^{M-1} h_{rsa}(i)\Delta V(t - i - T_{rsa}) + \sum_{i=0}^{M-1} h_{abr}(i)\Delta SBP(t - i - T_{abr}) + w_{RR}(t) \quad (1)$$

where T_{rsa} and T_{abr} are the latencies associated with the RSA and arterial baroreflex mechanisms, respectively, and $w_{RR}(t)$ represents the stochastic component of $\Delta RR(t)$ plus any contributions not accounted for by these two mechanisms. The

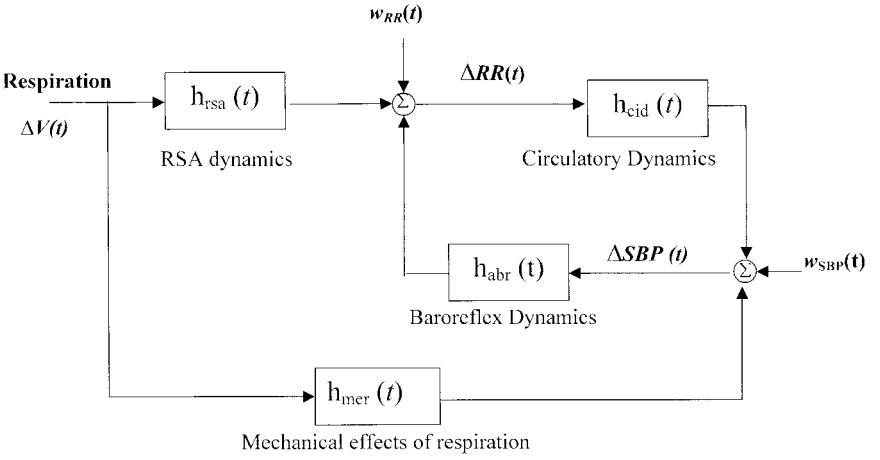

Fig. 1. Schematic block diagram of the closed-loop model of circulatory control. $\Delta V(t)$, fluctuation in respiration coupling; $h_{rsa}(t)$, respiratory sinus arrhythmia (RSA) impulse response; $w_{RR}(t)$, stochastic component of R-R intervals (RR); $\Delta RR(t)$, fluctuations in RR; $h_{cid}(t)$, impulse response in circulatory dynamics; $h_{abr}(t)$, baroreflex impulse response; $\Delta SBP(t)$, fluctuations in stochastic blood pressure; $w_{SBP}(t)$, stochastic influences on SBP; and $h_{mer}(t)$, response of mechanical effects on respiration.

model is assumed to be linear, and thus complete characterizations of RSA and baroreflex dynamics are given by their respective impulse responses. The baroreflex impulse response [$h_{abr}(t)$], for instance, quantifies the time course of the change in RR resulting from an abrupt increase in SBP of 1 mmHg. The RSA impulse response [$h_{rsa}(t)$] may be considered as reflecting the time course of the fluctuation in RR after a very rapid inspiration and expiration of 1 liter of air. These impulse responses are assumed to persist for a maximum duration of M sampling intervals. On the basis of the lengths of our datasets and preliminary analyses, we found 90 to be a suitable choice for M.

A portion of $\Delta SBP(t)$ is assumed to be produced by changes in intrathoracic pressure resulting from respiration; we will refer to this mechanism as the mechanical effect of respiration (MER). Fluctuations in heart rate may be expected to produce changes in SBP through variations in cardiac output as a consequence of the Frank-Starling mechanism and windkessel runoff (2, 11). We have labeled the totality of these effects circulatory dynamics (CID). These model assumptions take the following mathematical formulation

$$\Delta SBP(t) = \sum_{i=0}^{M-1} h_{cid}(t)\Delta RR(t - i - T_{cid}) + \sum_{i=0}^{M-1} h_{mer}(i)\Delta V(t - i) + w_{SBP}(t) \quad (2)$$

where T_{cid} is the latency associated with CID, and $w_{SBP}(t)$ represents stochastic and other influences on SBP not explained by the model. Details of the estimation procedure are given in the APPENDIX.

Statistical analysis. To facilitate the statistical comparison of the estimated impulse responses between and within subjects, we derived scalar descriptors representing the properties related to gain and time course of each response. There were several descriptors. First, impulse response magnitude (IRM) was computed as the difference between the maximum and minimum values of the estimated impulse response. Second, dynamic gain (DG) was computed by first taking the fast Fourier transform of the estimated impulse response to obtain the corresponding transfer function and calculating the average of the transfer function gains between 0.04 and 0.45 Hz. This range covers the span of frequencies pertinent to heart rate and blood pressure variability. Third, characteristic time (τ_c) provided a measure of the latency after which the bulk of the impulse response occurs and was defined as

$$\tau_c = \frac{\sum_{t=0}^{M-1} t|h(t)|}{\sum_{t=0}^{M-1} h(t)} \quad (3)$$

The summary cardiovascular measures that were extracted from the data and subjected to statistical analysis were mean RR, RR variability (i.e., standard deviation of RR about the mean), mean SBP, SBP variability (i.e., standard deviation of SBP), mean DBP, and DBP variability (i.e., standard deviation of DBP). In addition, two measures of baroreflex sensitivity (BRS), based on the spontaneous variability of SBP and RR, were computed for comparison with the baroreflex gain estimated from the model. The first, BRS_{seq}, was assessed using the sequence method. Here, the ratios between short (3–4 beats) increases/decreases in SBP and corresponding or subsequent increases/decreases in RR were computed and averaged (30, 31). The second, BRS_α, was computed from the power spectra of SBP and RR in the following manner (30)

$$BRS_\alpha = \frac{\sqrt{(P_{RR}/P_{SBP})_{LF}} + \sqrt{(P_{RR}/P_{SBP})_{HF}}}{2} \quad (4)$$

where P_{RR} and P_{SBP} represent the spectral powers of RR and SBP, respectively, in the low-frequency (0.04–0.15 Hz) and high-frequency (0.15–0.45 Hz) bands.

Before statistical testing, each of the aforementioned descriptors was tested for normality. If the normality assumption was not satisfied, log transformation was performed. Statistical analysis consisted of two-way repeated-measures analysis of variance, with the repeated factor being treatment condition (preCPAP vs. postCPAP) and the other factor being subject group (C vs. N). Because the subject groups were small and there was significant variability in CPAP use across individuals, we also applied correlation analysis to the pooled data from both groups. Here the Pearson correlation coefficient (r) between average nightly CPAP use and each model parameter or summary cardiovascular measure was computed. The estimated parameters for the baroreflex model component were also tested for correlation with BRS_{seq} and BRS_α. All statistical procedures were implemented using SigmaStat for Windows software (SPSS; Chicago, IL). The level of significance was set at $P = 0.05$. Numerical results are expressed as means ± SE, unless otherwise stated.

Goodness-of-fit between the model predictions and measurements was assessed by computing multiple coherence functions (4) for RR variability and SBP variability, respectively. A multiple coherence value of unity at all frequencies indicates perfect replication of the measured output by the model, whereas a value close to zero would mean that the model has no predictive value. The multiple coherence function for RR variability was computed in the following way. After estimation of $h_{rsa}(t)$ and $h_{abr}(t)$, *Eq. 1* was used to predict $\Delta RR(t)$. The power spectrum of predicted $\Delta RR(t)$ was subsequently calculated and then divided by the power spectrum of the measured $\Delta RR(t)$ on a frequency-by-frequency basis. The multiple coherence function for SBP variability was computed in a similar fashion, except that *Eq. 2* was used to predict $\Delta SBP(t)$.

RESULTS

Time series. A representative set of resampled time series of $\Delta V(t)$, $\Delta RR(t)$, and $\Delta SBP(t)$ measured from one of the subjects during the randomized breathing protocol is shown in Fig. 2. It should be noted from the $\Delta V(t)$ waveform that the larger breaths are associated with longer breath durations; this design helped in minimizing the breath-to-breath fluctuations in ventilation, and thus chemical drive. The immediate effects of respiration on $\Delta RR(t)$ and $\Delta SBP(t)$ are quite apparent. However, the presence of significantly lower frequency fluctuations, not related to the breathing pattern, is also clearly visible.

Changes in summary cardiovascular descriptors. The effects of long-term CPAP therapy on mean values of RR, SBP, and DBP, as well as the corresponding measures of variability, are summarized in Table 2. Repeated-measures ANOVA revealed no changes in

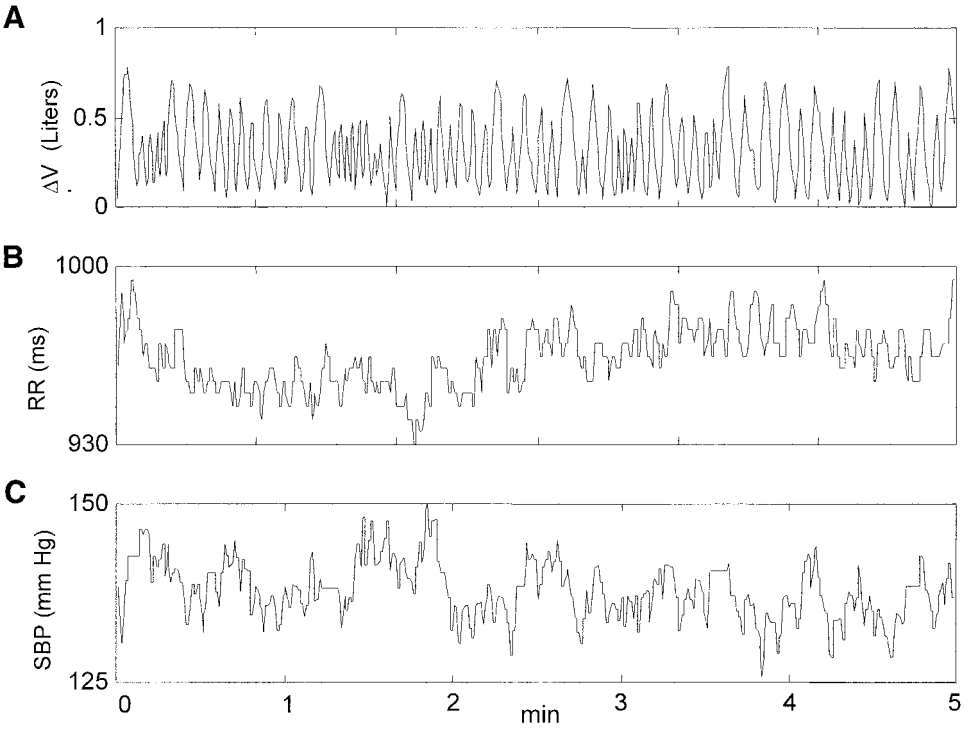

Fig. 2. Representative sample of the resampled signals for respiration (*A*), RR (*B*), and SBP (*C*) in one obstructive sleep apnea (OSA) subject during the randomized breathing protocol.

any of these measures, except for mean RR, which increased significantly ($P < 0.03$) in *group C* after CPAP therapy. The responses of the individual subjects are shown in Fig. 3. In *group C*, every subject demonstrated an increase in mean RR (or equivalently, a reduction in heart rate); in contrast, in *group N*, three subjects showed increases whereas the other four displayed a reduction in mean RR. The change in mean RR was significantly correlated with average nightly CPAP use (Table 2). None of the other summary cardiovascular measures showed any correlation with CPAP use.

Group-averaged impulse responses. The estimated group-averaged impulse responses for model components (RSA and baroreflex) that mediate RR variability are shown in Fig. 4 (*A* and C for *group C* and *B* and *D* for *group N*). Comparison of the PreCPAP and PostCPAP responses shows that long-term CPAP therapy produced dramatic increases in the magnitudes of the RSA and baroreflex impulse responses in *group C* but not in *group N*. The estimated group-averaged impulse responses for the model components (MER and CID) responsible for SBP variability are displayed in Fig. 5. CPAP therapy led to reductions in the MER and CID impulse responses in *group C* patients. In *group N*, the MER impulse response shows little change, whereas the CID impulse response displays an increase in magnitude in the followup study.

Multiple coherence values for RR variability and SBP variability were >0.5 between 0.15 and 0.25 Hz, demonstrating that the linear closed-loop model was able to account for >50% of the variance in the range of frequencies over which respiratory power was highest. This range largely coincides with the span of frequencies associated with the estimated impulse responses.

Table 2. *Effects of long-term CPAP therapy on heart rate and blood pressure*

	Two-way Repeated-Measures Analysis of Variance							Correlation Analysis
	Compliant subjects avg. nightly CPAP use >3 h		Noncompliant subjects, avg. nightly CPAP use <3 h		*P* value			
Parameter, units	PreCPAP	PostCPAP	PreCPAP	PostCPAP	Group	CPAP	Group × CPAP	Correlation with average nightly CPAP use (*P* value)
Mean RR, ms	764.2 ± 33.5	897.9 ± 55.6	751.1 ± 42.7	778.4 ± 61.0	0.324	0.006*	0.027*	0.642 (0.018)*
RR variability, ms	18.7 ± 4.0	31.8 ± 14.5	28.1 ± 5.5	27.3 ± 5.8	0.502	0.302	0.238	0.445 (0.128)
SBP, mmHg	114.9 ± 6.2	119.3 ± 9.5	107.9 ± 5.0	111.5 ± 4.1	0.395	0.360	0.938	0.097 (0.752)
SBP variability, mmHg	5.65 ± 0.62	4.79 ± 1.02	6.28 ± 0.59	7.11 ± 0.80	0.105	0.599	0.147	−0.272 (0.368)
DBP, mmHg	61.4 ± 6.0	57.3 ± 3.5	60.9 ± 4.5	55.8 ± 2.9	0.882	0.126	0.753	−0.126 (0.682)
DBP variability, mmHg	3.12 ± 0.28	2.32 ± 0.45	3.59 ± 0.47	3.08 ± 0.34	0.158	0.060	0.394	−0.163 (0.595)

Values are means ± SE. RR, R-R interval; BP, blood pressure; SBP, systolic BP; DBP, diastolic BP. Numbers in parentheses are average *P* values. *Statistically significant *P* values.

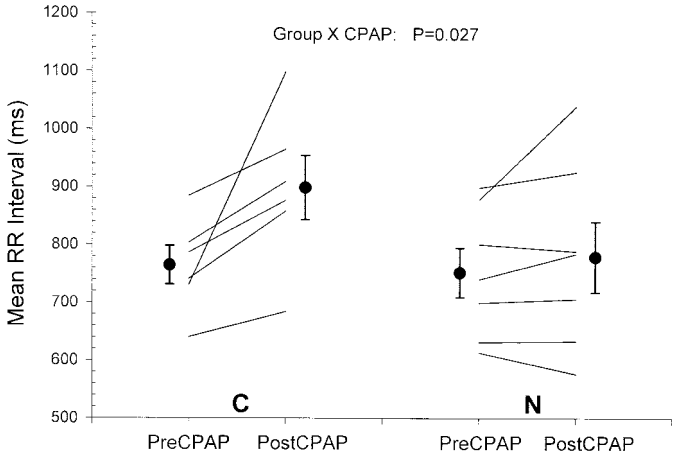

Fig. 3. Effect of long-term continuous positive airway pressure (CPAP) therapy on mean RR in the compliant (*group C*) patients and the noncompliant (*group N*) patients. Solid circles and error bars represent group means ± SE.

Changes in impulse response descriptors. Figure 6 displays the CPAP-induced changes in the individual and group-averaged values of the IRMs for all four model components. On average, the RSA and baroreflex IRMs increased almost threefold and MER IRM decreased by ~50% in *group C*, whereas there were no changes in the corresponding descriptors for *group N*. The group × treatment interaction was also significant in CID, but in this case, the *group C* subjects showed a decrease in IRM with CPAP whereas there was a tendency for the IRM to increase in *group N*. The group-averaged results for all three descriptors (IRM, DG, and τ_c) in each of the model components are summarized in Table 3. The results for DG closely paralleled those for IRM. On the other hand, there were no changes in τ_c for all four model components. As well, CPAP treatment did not produce any differences in any of the estimated model component delays. T_{abr} was 0.96 ± 0.17 s PreCPAP versus 0.85 ± 0.21 s postCPAP, whereas T_{rsa} was −0.88 ± 0.07 s PreCPAP versus −0.87 ± 0.06 s postCPAP.

The results of the correlation analysis generally supported the conclusions arrived at through analysis of variance. The gain parameters for the RSA, baroreflex, and CID model components were significantly correlated with average nightly CPAP use (Table 3). However, none of the descriptors of MER dynamics was significantly correlated with CPAP use.

Effects of CPAP on BRS. Although there was a tendency for BRS_{seq} to increase with CPAP therapy in

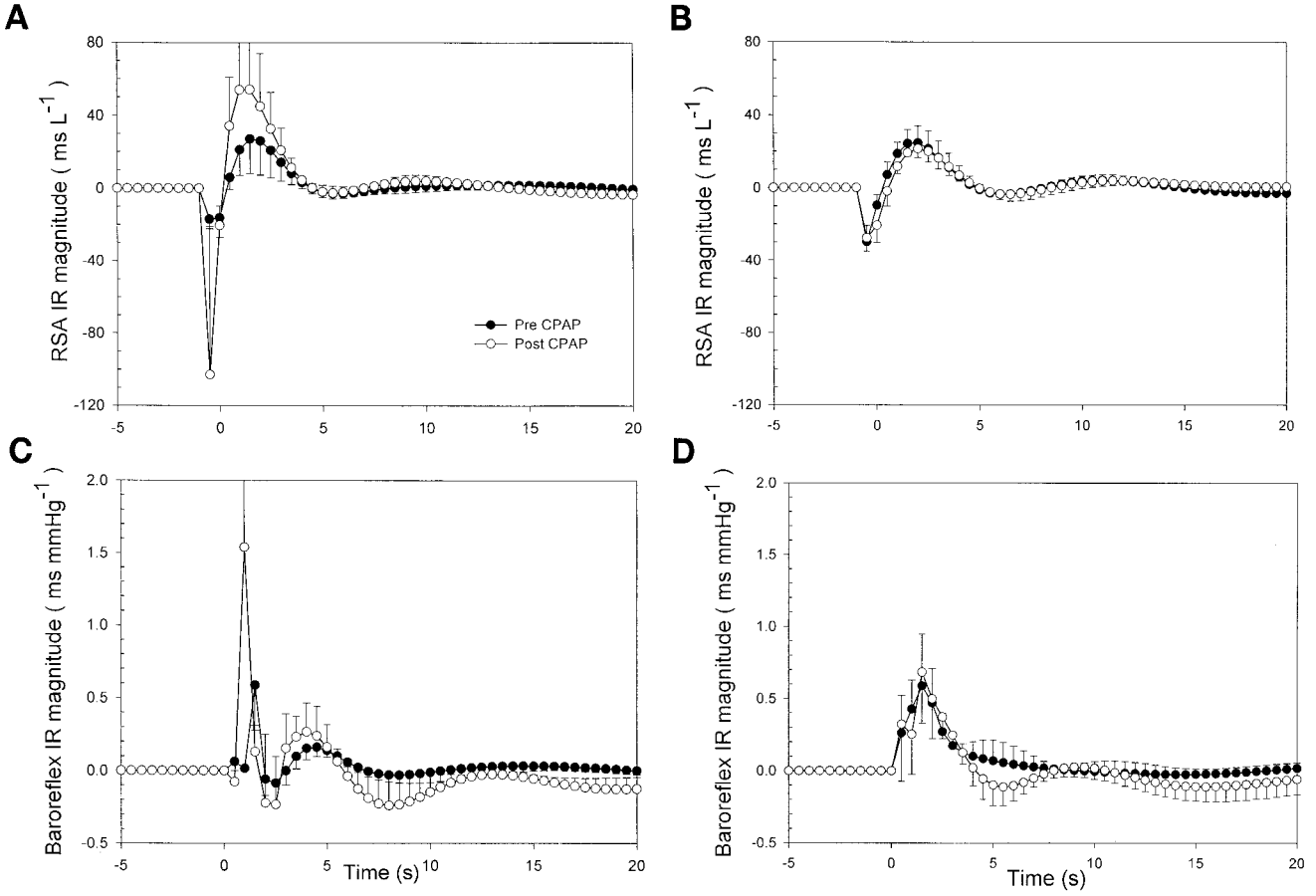

Fig. 4. Group-averaged impulse responses for the RSA and baroreflex model components in *group C* patients (*A* and *C*) and *group N* patients (*B* and *D*). Curves with solid circles represent impulse responses before CPAP therapy, whereas curves with open circles represent the corresponding postCPAP responses.

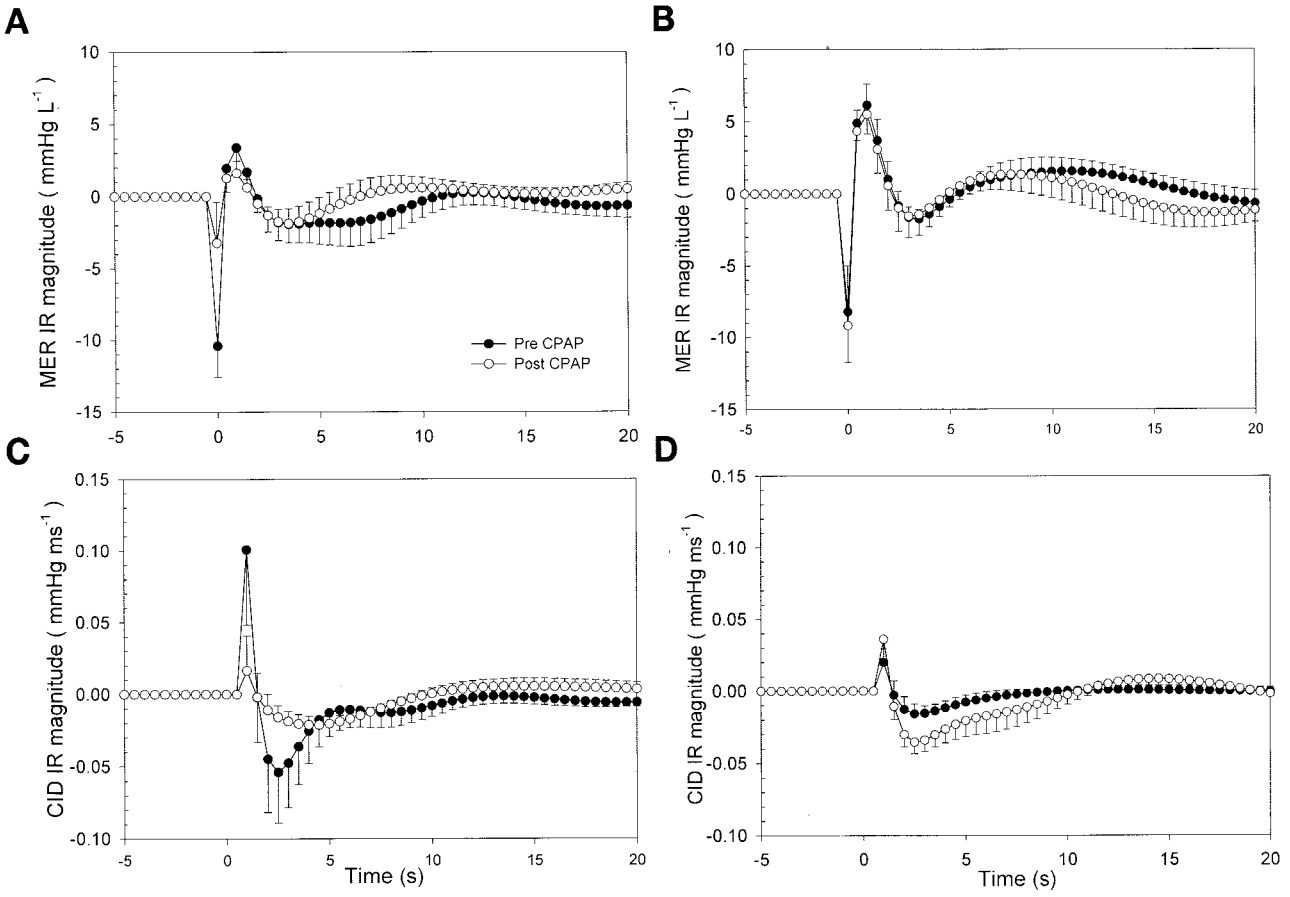

Fig. 5. Group-averaged impulse responses for model components mechanical effects in respiration (MER) and circulatory dynamics (CID) in *group C* patients (*A* and *C*) and *group N* patients (*B* and *D*). Curves with solid circles represent impulse responses before CPAP therapy, whereas curves with open circles represent the corresponding postCPAP responses.

group C (6.66 ± 0.32 preCPAP vs. 7.60 ± 0.62 postCPAP), the difference was not significant. There was clearly no change in BRS_{seq} in *group N* (7.11 ± 0.41 preCPAP vs. 7.17 ± 0.74 postCPAP). On the other hand, the preCPAP to postCPAP changes in BRS_{seq} in both groups were significantly correlated ($r = 0.68$, $P = 0.009$) with the corresponding changes in baroreflex IRM.

BRS_{α} increased significantly ($P = 0.018$) in *group C* with CPAP therapy (4.05 ± 1.23 preCPAP vs. 11.98 ± 7.05 postCPAP); in contrast, in *group N*, BRS_{α} was unchanged (6.15 ± 1.32 preCPAP vs. 5.29 ± 1.55 postCPAP). BRS_{α} was also significantly correlated ($r = 0.69$, $P = 0.008$) with baroreflex IRM.

DISCUSSION

A key feature of the analysis employed in this study is the imposition of causality on the model structure. This modeling constraint allows the unique estimation of the dynamic characteristics of the feedforward and feedback components that compose the closed-loop system, thus eliminating the need to "open the loop" with the use of pharmacological, surgical, or other invasive procedures. Similar approaches, with variations in model structure, have been employed in earlier studies (1, 2, 24, 25, 28) to investigate the autonomic control of heart rate and blood pressure. The present study, however, represents the first application of this model-based approach to determine the effect of CPAP therapy on circulatory control in OSA. It is also important to note that a major difference between our study and previous work lies in the mathematical formulation of the closed-loop model. In previous studies, a multivariate autoregressive model structure was assumed; in contrast, the impulse responses of our model components are constructed using Laguerre basis functions. The important practical advantage of this computational feature is that it can produce a substantial reduction in the number of unknown parameters that need to be estimated, thereby allowing greater statistical reliability to be achieved in the parameter estimates (21). Another advantage is that this approach introduces a certain amount of smoothing in the estimated impulse responses. However, the use of the Laguerre functions as a "shape factor" can lead to some bias in the estimates.

Apart from a reduction in mean heart rate, the conventional summary measures of HRV, mean blood pressure, and blood pressure variability in patients with OSA did not reveal any chronic effects of CPAP treatment. On the other hand, our closed-loop analysis

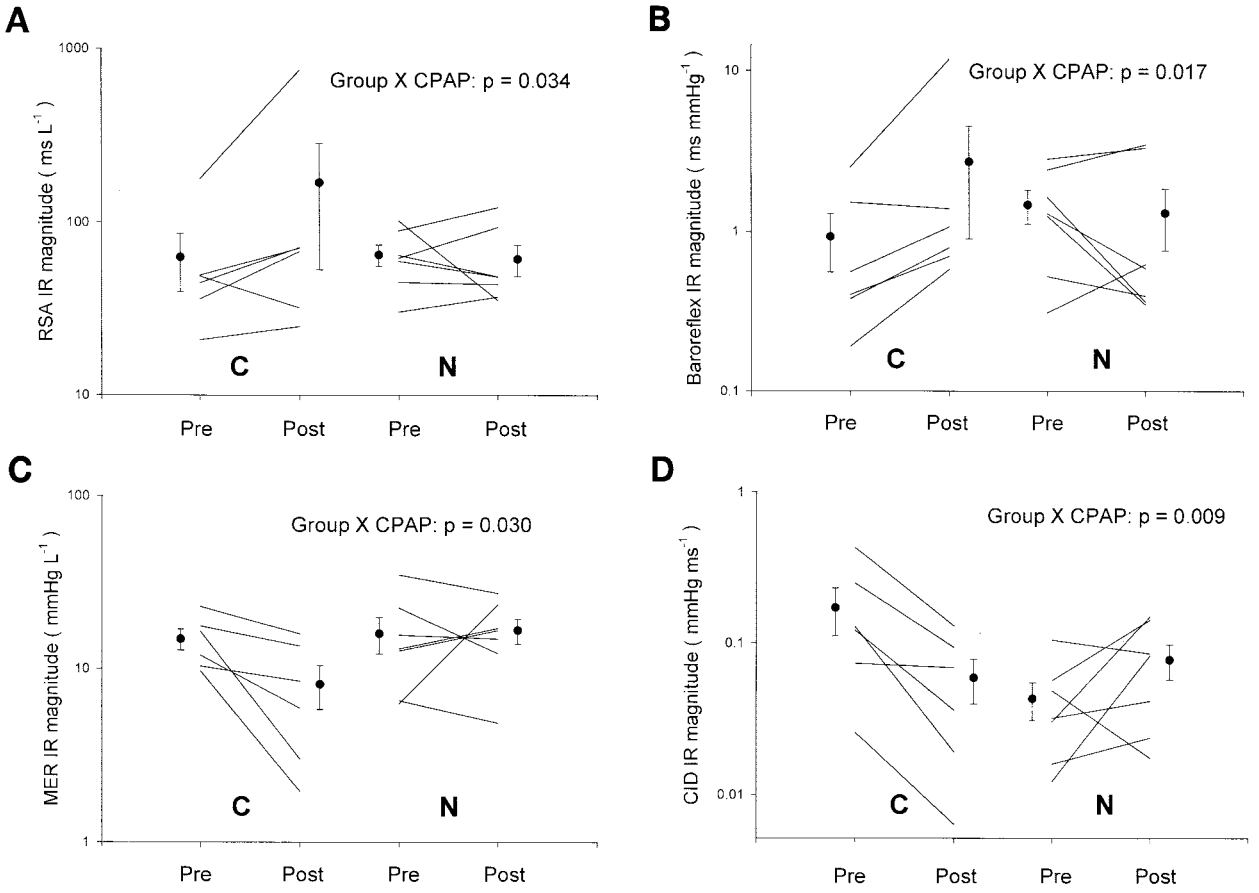

Fig. 6. Effect of CPAP therapy on impulse response magnitude (IRM) of the RSA (*A*), baroreflex (*B*), MER (*C*), and CID (*D*) model components.

Table 3. *Effects of long-term CPAP therapy on cardiorespiratory dynamics*

	Two-way Repeated-Measures ANOVA (Group × CPAP)							Correlation Analysis
	Compliant subjects, avg. nightly CPAP use >3 h		Noncompliant subjects, avg. nightly CPAP use <3 h		*P* value			
Parameter, units	PreCPAP	PostCPAP	PreCPAP	PostCPAP	Group	CPAP	Group × CPAP	Correlation with average nightly CPAP use, *P* value
RSA								
IR magnitude, ms/l	65.8 ± 28.4	196.7 ± 138.3	64.8 ± 9.3	61.2 ± 12.6	0.720	0.103	0.034*	0.612 (0.026)*
Dynamic gain, ms/l	101.1 ± 49.8	237.4 ± 160.1	95.6 ± 16.2	88.8 ± 21.8	0.806	0.250	0.058	0.553 (0.049)*
Characteristic time, s	13.8 ± 1.5	11.2 ± 2.1	9.9 ± 1.1	9.5 ± 1.0	0.131	0.242	0.375	−0.330 (0.271)
Baroreflex								
IR magnitude, ms/mmHg	0.92 ± 0.37	2.71 ± 1.81	1.46 ± 0.35	1.30 ± 0.54	0.917	0.374	0.017*	0.752 (0.003)*
Dynamic gain, ms/mmHg	1.02 ± 0.27	2.94 ± 1.71	2.09 ± 0.45	1.99 ± 0.76	0.582	0.266	0.028*	0.671 (0.012)*
Characteristic time, s	13.8 ± 0.9	12.9 ± 1.4	14.2 ± 0.9	13.4 ± 1.4	0.817	0.353	0.971	0.132 (0.668)
MER								
IR magnitude, mmHg/l	14.8 ± 2.1	8.1 ± 2.3	15.9 ± 3.8	16.6 ± 2.8	0.186	0.075	0.030*	−0.463 (0.111)
Dynamic gain, mmHg/l	18.6 ± 3.2	11.4 ± 2.7	18.2 ± 3.6	20.1 ± 1.9	0.279	0.290	0.055	−0.468 (0.107)
Characteristic time, s	13.9 ± 1.3	15.8 ± 0.8	14.2 ± 1.4	11.3 ± 1.3	0.060	0.729	0.128	0.522 (0.067)
CID								
IR magnitude, mmHg/ms	0.172 ± 0.060	0.060 ± 0.019	0.043 ± 0.011	0.077 ± 0.020	0.178	0.125	0.009*	−0.518 (0.070)
Dynamic gain, mmHg/ms	0.235 ± 0.070	0.098 ± 0.028	0.074 ± 0.018	0.124 ± 0.030	0.187	0.127	0.004*	−0.575 (0.040)*
Characteristic time, s	12.2 ± 0.8	13.3 ± 1.8	15.5 ± 0.9	12.3 ± 1.4	0.353	0.576	0.202	0.276 (0.361)

Values are means ± SE. RSA, respiratory sinus arrhythmia; MER, mechanical effects on respiration; CID, circulatory dynamics; IR, impulse response. *Statistically significant *P* values.

showed that adequate application of long-term CPAP therapy produces substantial alterations in the major physiological mechanisms that influence HRV and blood pressure variability. We believe that the greater sensitivity of our technique is because it quantifies the coupling between any two of the three measured physiological variables: respiration, heart rate, and blood pressure. For instance, we found that baroreflex gain increased roughly threefold in *group C* subjects after CPAP therapy; this change acting alone would have led to a substantial increase in HRV. However, RR variability did not increase significantly after CPAP (see Table 2). We believe that this is due to the corresponding decrease in CID gain, which cancelled out much of the effect of the gain increase around the baroreflex loop. Mukkamala et al. (24) arrived at a similar conclusion regarding the enhanced sensitivity of this kind of closed-loop analysis in a different clinical application. They demonstrated that the differences in cardiovascular control between control subjects and patients with diabetic autonomic neuropathy that were undetectable using standard autonomic tests became identifiable using closed-loop modeling. Mullen et al. (25) demonstrated the physiological validity of this closed-loop modeling approach to the extent that was achievable in normal humans. The authors found here that baroreflex and RSA gains estimated from their model became essentially zero after combined parasympathetic and β-sympathetic pharmacological blockade. O'Leary et al. (28) have also shown that orthostatic stress induced by head-up tilt leads to a substantial reduction in baroreflex gain, as estimated using a similar modeling approach.

Baroreflex gain, as quantified by estimates of IRM and DG for the baroreflex model component as well as BRS_{seq} and BRS_{α}, was substantially lower PreCPAP in the OSA patients, compared with the ranges reported for normals in the literature (30, 32). Our estimates of BRS_{seq} were similar in range to the values for untreated OSA subjects reported in previous studies (8, 31). After CPAP therapy, baroreflex gain increased almost threefold in *group C* subjects, although τ_c remained statistically unchanged. In contrast, *group N* subjects showed little change in baroreflex gain or time course. The changes in estimated baroreflex IRM and DG were significantly correlated with the corresponding changes in baroreflex sensitivity determined independently from the sequence and power spectral methods. On the other hand, the estimates of BRS_{seq} per se were not statistically different preCPAP versus postCPAP. A possible explanation for this discrepancy is that the estimates of BRS_{seq} are more susceptible to error than IRM or DG of the baroreflex component, because the sequence method does not take into account the confounding influences of respiration on heart rate and blood pressure. Tkacova et al. (40) recently reported CPAP-induced increases in BRS_{seq} in eight OSA patients during sleep; the increase in BRS_{seq} persisted during the second half of the night even after CPAP was withdrawn. However, all of the OSA patients studied by Tkacova et al. also had congestive heart failure, whereas in our study, none of our subjects had any known cardiovascular disease, except for hypertension in five of the patients. Another important difference is that Tkacova's study focused on the persisting effects of CPAP during sleep in the few hours after withdrawal of this therapy; in our study, we studied OSA patients during wakefulness after several months of nocturnal CPAP treatment.

As mentioned earlier, the RSA model component represents the autonomically mediated coupling between respiration and heart rate. Our estimated RSA impulse responses were biphasic in form, showing an initial decrease in RR (or acceleration of heart rate), followed by a subsequent RR increase (deceleration of heart rate). This dynamic behavior is compatible with the corresponding estimates that have been reported previously (24, 25). A key finding in this study is that RSA gain in *group C* subjects increased dramatically after CPAP therapy, whereas the corresponding descriptors were unchanged in *group N*. Because RSA dynamics are mediated largely through parasympathetic control, this finding is consistent with previous reports (17, 34) that acute and chronic application of CPAP in OSA patients led to increases in parasympathetic activity. These conclusions are also supported by our finding that mean heart rate was dramatically reduced in the *group C* subjects after CPAP therapy but remained unchanged in *group N*.

The CID model component represents the "feedforward" coupling (1) between changes in RR and changes in SBP. The dynamic behavior of the estimated CID impulse responses (Fig. 5) may be explained as follows. The immediate effect of an increase in RR is a decrease in the subsequent DBP; this has been termed the "runoff effect" (2). On the other hand, because of the increased time for filling, the subsequent stroke volume, and thus pulse pressure (= SBP−DBP), would increase, in accordance with the Frank-Starling law. The net effect could be a decrease or increase in the subsequent SBP, depending on the relative strengths of the runoff and Starling effects. In most of our subjects, the CID impulse response showed a brief initial (next-beat) increase, indicating the predominance of the Starling effect in these cases. This was followed subsequently by a more sustained decrease, reflecting the effect of a reduction in cardiac output produced by the lowered heart rate. The extent to which the change in cardiac output translates into a corresponding change in SBP is determined largely by the peripheral resistance. In *group C* subjects, long-term CPAP therapy led to substantial reductions in CID gain, whereas in *group N* patients, this parameter tended to increase. Based on our understanding of the mechanisms involved, we believe that these changes in CID dynamics reflect a decrease in peripheral resistance after CPAP therapy in *group C* and an increased peripheral resistance in some of the *group N* subjects. These conclusions are consistent with previous work showing that sympathetic activity decreased in OSA patients only if

CPAP therapy was applied for an extended duration and compliance with treatment was high (23).

The dynamic behavior of the estimated MER model component was also similar in form to previously reported results (2, 24, 25). Immediately after the start of inspiration, there is an abrupt drop in blood pressure as a consequence of the decreased (i.e., more negative) intrathoracic pressure. Subsequently, however, the decreased intrathoracic pressure during inspiration promotes increased diastolic filling, which also raises DBP and SBP. During expiration, intrathoracic pressure becomes less negative, thereby negating the earlier increase in SBP. The mechanical effect of respiration on SBP thus depends on the amplitude of the resulting change in amplitude of intrathoracic pressure. The intrathoracic pressure swing that results from a given tidal volume, in turn, depends on lung volume and/or lung compliance. One likely interpretation of our finding of a postCPAP decrease in MER IRM and DG in *group C* patients is that long-term CPAP therapy led to increased resting lung volume and/or lung compliance, thereby reducing the intrathoracic pressure swing per unit volume of air inspired. This explanation is not unreasonable because it has been shown (6) that end-expiratory volume increases during CPAP and remains elevated after CPAP withdrawal in patients with congestive heart failure. Another study (39) has shown a reduction in intrathoracic pressure swings during CPAP and that this reduction persists after CPAP withdrawal, suggesting a CPAP-induced increase in lung compliance.

One strength of the present study is that compliance with the prescribed CPAP therapy was measured objectively by means of a built-in microchip that stored the time at which the CPAP device was used at the physician-assigned pressure. This contrasts with some previous studies (27, 34), in which CPAP compliance was either not disclosed or based on self-reported estimated use. It is well known that self-reported use of CPAP tends to exceed true use (18). On the other hand, an important weakness of our study design is the use of the noncompliant patients as the "control" group, because the subjects who ended up in this group were not randomly preselected. Clearly, it would have been preferable from a statistical standpoint to compare the treated patients with a control group of matched subjects who were not administered any CPAP therapy over the study duration. On the other hand, there were no significant differences in age, body mass index, apnea-hypopnea index, or prescribed CPAP levels between the *group C* and *group N* subjects. Nor were there significant differences between the subject groups in mean heart rate, mean blood pressures, HRV, and blood pressure variability or any of the model-based descriptors.

Another limitation of the present study is that the randomized breathing protocol required subject cooperation and mental concentration. Substantial mental stress has been shown to reduce baroreflex sensitivity (37) and RSA magnitude (29). On the other hand, Cooke et al. (10) found no appreciable changes in cardiovascular autonomic function when their subjects switched from uncontrolled to controlled breathing protocols. In our study, we attempted to minimize the mental stress associated with the randomized breathing procedure by allowing the subjects to perform one or two practice runs before actual data collection; furthermore, the randomized breathing protocol was limited to 5 min in duration. If mental effort affected our results, it is likely that the effect was small or uniformly spread among the subjects because the differences in estimated model component responses between *groups C* and *N* were clearly substantial. To explore this issue further, we applied our method of analysis to data segments recorded before the start of the randomized breathing protocol, during which the subjects were breathing spontaneously. Comparison of the estimates of baroreflex and RSA gains computed from these spontaneous breathing segments to corresponding segments in which the subjects tracked the randomized pattern showed no significant differences. For instance, the mean changes in baroreflex IRM from spontaneous breathing to randomized breathing were indistinguishable from zero: 0.43 ± 0.36 ms/mmHg ($P = 0.26$) preCPAP and 0.26 ± 0.71 ms/mmHg ($P = 0.72$) postCPAP. The corresponding mean changes in RSA IRM from spontaneous breathing to randomized breathing were also not significantly different from zero: 27.2 ± 20.1 ms/l ($P = 0.20$) preCPAP and −6.6 ± 26.9 ms/l ($P = 0.81$) postCPAP. However, in making these comparisons, one should keep in mind that the model estimates obtained during spontaneous breathing were associated with larger estimation errors, due to the narrow-band frequency spectrum of the respiratory input (3).

A further weakness in our study design is that we did not monitor end-tidal P_{CO_2}. It is possible that arterial blood gases and thus chemoreflex drive may have been altered during the randomized breathing protocol. However, computation of the average minute ventilation (during randomized breathing) showed that it remained unchanged in each subject between the preCPAP and postCPAP studies. In *group C* subjects, ventilation was 6.3 ± 0.5 l/min preCPAP versus 7.4 ± 0.7 l/min postCPAP; in *group N*, the corresponding values were 7.2 ± 0.9 l/min preCPAP versus 7.2 ± 0.8 l/min postCPAP. Thus it is highly unlikely that differences in chemoreflex drive were an important contributor to the differences in autonomic function detected by our model.

In conclusion, our proposed model-based approach represents a relatively nonintrusive means of assessing the multiple facets of autonomic control of heart and blood pressure in OSA patients from a single test procedure. Our findings indicate that long-term CPAP therapy can lead to a substantial elevation of baroreflex sensitivity and RSA gain in OSA patients. In addition to improvements in the autonomic reflexes, CPAP therapy also appears to alter nonneural mechanisms such as the mechanical effects of respiration on arterial blood pressure and the feedforward effect of fluctuations in heart rate on fluctuations in blood pres-

sure, but the physiological bases of these effects remain unclear. However, improvements in both the autonomically mediated and nonneural mechanisms of circulatory control depend strongly only whether there is adequate compliance with the prescribed treatment.

APPENDIX

Estimation of model impulse responses. Each of the unknown impulse responses were expanded as the sum of several weighted Laguerre basis functions (21). For instance, in the case of the baroreflex and RSA model components

$$h_{\mathrm{abr}}(t) = \sum_{j=0}^{q_{\mathrm{abr}}-1} c_j^{\mathrm{abr}} \mathrm{L}_j(t) \qquad (A1)$$

$$h_{\mathrm{rsa}}(t) = \sum_{j=0}^{q_{\mathrm{rsa}}-1} c_j^{\mathrm{rsa}} \mathrm{L}_j(t) \qquad (A2)$$

where the $\mathrm{L}_j(t)$ represents the jth-order discrete-time orthonormal Laguerre function, and c_j^{abr} and c_j^{rsa} are the corresponding unknown weights that are assigned to $\mathrm{L}_j(t)$ in the baroreflex and RSA impulse responses, respectively. $\mathrm{L}_j(t)$ is defined as follows over the interval $0 \leq t \leq M-1$

$$\mathrm{L}_0(t) = \sqrt{\alpha^t(1-\alpha)} \qquad (A3)$$

and

$$\mathrm{L}_j(t) = \sqrt{\alpha}\mathrm{L}_j(t-1) + \sqrt{\alpha}\mathrm{L}_{j-1}(t) - \mathrm{L}_{j-1}(t-1), \quad 0 \leq j \leq q_{\mathrm{abr}}, q_{\mathrm{rsa}} \qquad (A4)$$

In *Eqs. A3* and *A4*, the parameter α ($0 < \alpha < 1$) determines the rate of exponential decline of the Laguerre functions and is selected such that, for given M, q_{rsa}, and q_{abr}, the values of the constructed impulse response become insignificant as t approaches M. Substituting *Eqs. A1* and *A2* into *Eq. 1*, we obtain, after some algebraic manipulation

$$\Delta\mathrm{RR}(t) = \sum_{j=0}^{q_{\mathrm{rsa}}-1} c_j^{\mathrm{rsa}} u_j(t) + \sum_{j=0}^{q_{\mathrm{abr}}-1} c_j^{\mathrm{abr}} v_j(t) + w_{\mathrm{RR}}(t) \qquad (A5)$$

where $u_j(t)$ and $v_j(t)$ are new derived variables, defined as follows

$$u_j(t) = \sum_{i=0}^{M-1} \mathrm{L}_j(i)\Delta V(t-i-T_{\mathrm{rsa}}) \qquad (A6)$$

$$v_j(t) = \sum_{i=0}^{M-1} \mathrm{L}_j(i)\Delta\mathrm{SBP}(t-i-T_{\mathrm{abr}}) \qquad (A7)$$

Equation A5 becomes the new linear relation with unknown parameters $c_j^{\mathrm{rsa}}(0 \leq j \leq q_{\mathrm{abr}})$ and c_j^{abr} $(0 \leq j \leq q_{\mathrm{rsa}})$ that can be estimated using least-squares minimization. However, note that *Eq. A5* contains far fewer unknown parameters ($q_{\mathrm{rsa}} + q_{\mathrm{abr}} \ll 2M$) than *Eq. 1*. A similar approach was applied to *Eq. 2*.

The least-squares minimization procedure described above was repeated for a range of values for the delays (T_{rsa}, T_{abr}, and T_{cid}) and Laguerre function orders (q_{abr}, q_{rsa}, q_{cid}, and q_{mer}). For each combination of delays and Laguerre function orders, a metric of the quality of fit, known as the minimum description length (MDL), was computed (33). MDL was computed as

$$\mathrm{MDL} = \log(J_R) + \frac{\text{total no. of parameters} \times \log(M)}{M} \qquad (A8)$$

where J_R is the variance of the residual errors between the measured data and the predicted output. Note that MDL decreases as J_R decreases but increases with increasing model order. Selection of the "optimal" candidate model was based on a global search for the minimum MDL; in addition, this optimal solution had to satisfy the condition that the cross-correlations between the residual errors and past values of the two inputs [$\Delta V(t)$ and $\Delta\mathrm{SBP}(t)$ in the case of *Eq. 1*, and $\Delta V(t)$ and $\Delta\mathrm{RR}(t)$ in *Eq. 2*] had to be not significantly different from zero. Once the optimal parameter values were determined, the impulse responses of the four model components were computed by using *Eqs. A1*, *A2*, and the analogous equations for MER and CID. q_{abr}, q_{rsa}, q_{cid}, and q_{mer} each ranged from 6 to 8.

Because a closed-loop structure was inherent in the model, it was necessary to impose causality constraints in an explicit fashion during the parameter estimation procedure. In the estimation of baroreflex dynamics, a minimum value of 0.5 s (i.e., 1 sampling interval) was assumed for T_{abr}, reflecting the fact that latencies are present in the baroreception process. In the case of the CID component, we assumed $T_{\mathrm{cid}} = 1$ s to ensure that a change in the current RR can affect pulse pressure, and thus SBP, only in the following beat (Starling effect). Previous reports (24, 25) have demonstrated an apparent noncausal relationship between $\Delta V(t)$ and $\Delta\mathrm{RR}(t)$, in which changes in heart rate precede changes in lung volume. A reasonable explanation for this observation is that, although there is simultaneous neural modulation of heart rate and the drive to breathe, mechanical inspiration takes effect later. Thus we allowed T_{rsa} to assume negative values. Finally, for MER dynamics, we allowed for the possibility that the mechanical effect of respiration on blood pressure could be virtually instantaneous; hence, no delay was assumed in this case.

We thank Edwin Valladares for technical assistance.

This study was supported by National Institutes of Health Grants HL-58725 and RR-01861.

REFERENCES

1. **Barbieri R, Parati G, and Saul JP.** Closed-versus open-loop assessment of heart rate baroreflex. *IEEE Eng Med Biol Mag* 20: 33–42, 2001.
2. **Baselli G, Cerutti S, Civardi S, Malliani A, and Pagani M.** Cardiovascular variability signals: towards the identification of a closed-loop model of the neural control mechanisms. *IEEE Trans Biomed Eng* 35: 1033–1045, 1988.
3. **Belozeroff V.** *A Model of Cardiorespiratory Autoregulation in Obstructive Sleep Apnea Syndrome* (PhD thesis). Los Angeles, CA: Univ. of Southern California, 2001.
4. **Bendat JS and Piersol AG.** *Engineering Applications of Correlation and Spectral Analysis*. New York: Wiley, 1980, p. 195–197.
5. **Berger RD, Akselrod S, Gordon D, and Cohen RJ.** An efficient algorithm for spectral analysis of heart rate variability. *IEEE Trans Biomed Eng* 33: 900–904, 1986.
6. **Butler GC, Naughton MT, Rahman MA, Bradley TD, and Floras JS.** Continuous positive airway pressure increases heart rate variability in congestive heart failure. *J Am Coll Cardiol* 25: 672–679, 1995.
7. **Carlson JT, Hedner J, Elam M, Ejnell H, Sellgren J, and Wallin BG.** Augmented resting sympathetic activity in awake patients with obstructive sleep apnea. *Chest* 103: 1763–1768, 1993.

8. **Carlson JT, Hedner JA, Sellgren J, Elam M, and Wallin G.** Depressed baroreflex sensitivity in patients with OSA. *Am J Respir Crit Care Med* 154: 1490–1496, 1996.
9. **Carskadon MA and Rechtshaffen A.** Montoring and staging human sleep. In: *Principles and Practice of Sleep Medicine*, edited by Kryger MH, Roth T, and Dement WC. Philadelphia, PA: Saunders, 1989, p. 665–683.
10. **Cooke WH, Cox JF, Diedrich AM, Taylor JA, Beightol LA, Ames JEIV, Hoag JB, Seidel H, and Eckberg DL.** Controlled breathing protocols probe human autonomic cardiovascular rhythms. *Am J Physiol Heart Circ Physiol* 274: H709–H718, 1998.
11. **DeBoer RW, Karemaker JM, and Strackee J.** Hemodynamic fluctuations and baroreflex sensitivity in humans: a beat-to-beat model. *Am J Physiol Heart Circ Physiol* 253: H680–H689, 1987.
12. **Dimsdale JE, Coy T, Ziegler MG, Ancoli-Israel S, and Clausen J.** The effect of sleep apnea on plasma and urinary catecholamines. *Sleep* 18: 377–381, 1995.
13. **Engleman HM, Martin SE, Deary IJ, and Douglas NJ.** Effect of continuous positive airway pressure treatment on daytime function in sleep apnoea/hypopnea syndrome. *Lancet* 343: 572–575, 1994.
14. **Hedner J, Darpo B, Ejnell H, Carlson J, and Caidahl K.** Reduction in sympathetic activity after long-term CPAP treatment in sleep apnoea: cardiovascular implications. *Eur Respir J* 8: 222–229, 1995.
15. **Hers V, Liistro G, Dury M, Collard P, Aubert G, and Rodenstein DO.** Residual effect of CPAP applied for part of the night in patients with obstructive sleep apnea. *Eur Respir J* 10: 973–976, 1997.
16. **Khoo MCK, Kim TS, and Berry RB.** Spectral indices of cardiac autonomic function in obstructive sleep apnea. *Sleep* 22: 443–451, 1999.
17. **Kim TS and Khoo MCK.** Estimation of cardiorespiratory transfer under spontaneous breathing conditions: a theoretical study. *Am J Physiol Heart Circ Physiol* 273: H1012–H1023, 1997.
18. **Kribbs NB, Kline LR, Pack AI, Smith PL, Swartz AR, Schubert NM, Redline S, Getsy JE, Henry JN, and Dinges DF.** Objective measurements of nasal CPAP treatment for obstructive sleep apnea: patterns of use and comparison to patient reports. *Am Rev Respir Dis* 147: 887–895, 1993.
19. **Malliani A, Pagani M, Lombardi F, and Cerutti S.** Cardiovascular neural regulation explored in the frequency domain. *Circulation* 84: 482–492, 1991.
20. **Mancia G, Grassi G, Daffonchio A, and Parati G.** Evaluating sympathetic activity in human hypertension. *J Hypertens* 11 *Suppl*: S13–S19, 1993.
21. **Marmarelis VZ.** Identification of nonlinear biological systems using Laguerre expansion of kernels. *Ann Biomed Eng* 21: 573–589, 1993.
22. **Mayer J, Becher H, Brandengurg U, Penzel T, Peter JH, and von Wichert P.** Blood pressure and sleep apnea: results of long-term nasal continuous positive airway pressure therapy. *Cardiology* 79: 84–92, 1991.
23. **McArdle N, Devereux G, Heidarnejad H, Engleman HM, MacKay TW, and Douglas NJ.** Long-term use of CPAP therapy for sleep apnea/hypopnea syndrome. *Am J Respir Crit Care Med* 159: 1108–1114, 1999.
24. **Mukkamala R, Mathias JM, Mullen TJ, Cohen RJ, and Freeman R.** System identification of closed-loop cardiovascular control mechanisms: diabetic autonomic neuropathy. *Am J Physiol Regulatory Integrative Comp Physiol* 276: R905–R912, 1999.
25. **Mullen TJ, Appel ML, Mukkamala R, Mathias JM, and Cohen RJ.** System identification of closed-loop cardiovascular control: effects of posture and autonomic blockade. *Am J Physiol Heart Circ Physiol* 272: H448–H461, 1997.
26. **Narkiewicz K, Montano N, Cogliati C, van de Borne PJH, Dyken ME, and Somers VK.** Altered cardiovascular variability in obstructive sleep apnea. *Circulation* 98: 1071–1077, 1998.
27. **Narkiewicz K, Masahiko K, Phillips BG, Pesek CA, Davison DE, and Somers VK.** Nocturnal continuous positive airway pressure decreases daytime sympathetic traffic in obstructive sleep apnea. *Circulation* 100: 2332–2335, 1999.
28. **O'Leary DD, Lin DC, and Hughson RL.** Determination of baroreflex gain using auto-regressive moving-average analysis during spontaneous breathing. *Clin Physiol* 5: 369–377, 1999.
29. **Patwardhan AR, Vallurupalli S, Evans JM, Bruce EN, and Knapp CF.** Override of spontaneous respiratory pattern generator reduces cardiovascular parasympathetic influence. *J Appl Physiol* 79: 1048–1054, 1995.
30. **Parati G, Di Rienzo M, and Mancia G.** How to measure baroreflex sensitivity: from the cardiovascular laboratory to daily life. *J Hypertens* 18: 7–19, 2000.
31. **Parati G, Di Rienzo M, Bonsignore MR, Insalaco G, Marrone O, Castiglioni P, Bonsignore G, and Mancia G.** Autonomic cardiac regulation in obstructive sleep apnea syndrome: evidence from spontaneous baroreflex analysis during sleep. *J Hypertens* 15: 1621–1626, 1997.
32. **Patton DJ, Triedman JK, Perrott MH, Vidian AA, and Saul JP.** Baroreflex gain: characterization using autoregressive moving average analysis. *Am J Physiol Heart Circ Physiol* 270: H1240–H1249, 1996.
33. **Rissanen J.** Estimation of structure by minimum description length. *Circ Syst Sig Process* 1: 395–406, 1982.
34. **Roche F, Court-Fortune I, Pichot V, Duverney D, Costes F, Emonot A, Vergnon JM, Geyssant A, Lacour JR, and Barthelemy JC.** Reduced cardiac sympathetic autonomic tone after long-term nasal continuous positive airway pressure in obstructive sleep apnoea syndrome. *Clin Physiol* 19: 127–134, 1999.
35. **Roux F, D'Amrosio C, and Mohsenin V.** Sleep-related breathing disorders and cardiovascular disease. *Am J Med* 108: 396–402, 2000.
36. **Somers VK, Dyken ME, Clary MP, and Abboud FM.** Sympathetic neural mechanisms in obstructive sleep apnea. *J Clin Invest* 96: 1897–1904, 1995.
37. **Steptoe A and Sawada Y.** Assessment of baroreflex function during mental stress and relaxation. *Psychophysiology* 26: 140–147, 1989.
38. **Task Force of the European Society of Cardiology and the North American Society of Pacing and Electrophysiology.** Heart rate variability: standards of measurement, physiological interpretation and clinical use. *Circulation* 93: 1043–1065, 1996.
39. **Tkacova R, Rankin F, Fitzgerald F, Floras JS, and Bradley TD.** Effects of continuous positive airway pressure on obstructive sleep apnea and left ventricular afterload in patients with heart failure. *Circulation* 98: 2269–2275, 1998.
40. **Tkacova R, Dajani HR, Rankin F, Fitzgerald FS, Floras JS, and Bradley TD.** Continuous positive airway pressure improves nocturnal baroreflex sensitivity of patients with heart failure and obstructive sleep apnea. *J Hypertens* 18: 1257–1262, 2000.
41. **Veale D, Pepin JL, Wuyam B, and Levy PA.** Abnormal autonomic stress responses in obstructive sleep apnoea are reversed by nasal continuous positive airway pressure. *Eur Respir J* 9: 2122–2126, 1996.
42. **Waravdekar NV, Sinoway LI, Zwillich CW, and Leuenberger UA.** Influence of treatment on muscle sympathetic nerve activity in sleep apnea. *Am J Respir Crit Care Med* 153: 1333–1338, 1996.
43. **Weiss JW, Launois SH, and Anand A.** The acute hemodynamic response to upper airway obstruction during sleep. In: *Sleep Apnea: Implications in Cardiovascular and Cerebrovascular Disease*, edited by Bradley TD and Floras JS. New York: Dekker, 2000, p. 213–226.
44. **Zwillich CW.** Is untreated sleep apnea a contributing factor for chronic hypertension? *JAMA* 283: 1880–1881, 2000.